A Ring-based Tyre Model for the Prediction of Structure-borne Interior Tyre/Road Noise

P. Kindt, P. Sas, W. Desmet

Katholieke Universiteit Leuven, Dept. Mechanical Engineering, Belgium, Email: peter.kindt@mech.kuleuven.be

Introduction

The increasing awareness for tyre/road noise and the resulting tyre/road noise reduction targets have increased the need for more accurate simulation tools. A wide range of tyre models are available, ranging from physical to statistical models. However, there is still a lack of computationally efficient physical tyre models that are based on a simple parameterization procedure for the prediction of structure-borne tyre/road noise [1].

The structural finite element tyre model presented in this paper is based on a three-dimensional flexible ring on an elastic foundation. The ring represents the treadband and the elastic foundation represents the tyre sidewall. The model is valid below the first treadband axial bending mode and includes a model of the wheel and the air cavity. For the 205/55R16 tyre used in this paper, the model is valid up to 300 Hz. This makes the model suitable for the prediction of structure-borne vehicle interior noise. Unlike most ring models which consider only in-plane motion, the presented model also predicts modes that involve torsion of the belt in circumferential direction. The parameterization is based on the main geometrical properties of the tyre and a limited modal test on an unloaded tyre.

Analytical ring model

The dynamic behaviour of a radial-belted tyre can be described approximately by a flexible ring on an elastic foundation (Figure 1). The sidewall stiffness of the presented tyre model is calculated from the analytical expression of the natural frequencies of a flexible ring on an elastic foundation. The effect of the circumferential tension in the ring due to the internal pressure is taken into account during the derivation of the expression for the natural frequencies.

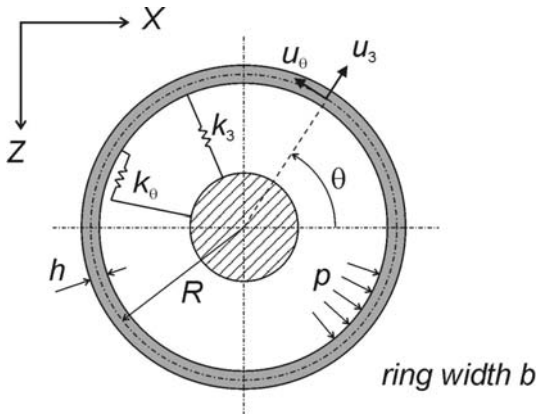

Figure 1: Flexible ring on elastic foundation with internal pressure.

Equations of motion

The displacements u_3 and u_θ are the radial and tangential displacement of the neutral surface, respectively. The neutral surface is referred to as the surface where the stresses are of a membrane type; bending stresses are zero in the neutral surface. All displacements are considered to be constant over the belt width. The radius, thickness, width and density of the ring are R, h, b and ρ, respectively. The inner surface of the ring is subjected to a pressure p (Pa). k_3 and k_θ are the stiffness values per unit area (N/m³) of the distributed radial and tangential linear springs. The equations of motion for the ring are [2]:

$$\frac{D}{R^4}\left(\frac{\partial^2 u_\theta}{\partial\theta^2}-\frac{\partial^3 u_3}{\partial\theta^3}\right)+\frac{K}{R^2}\left(\frac{\partial^2 u_\theta}{\partial\theta^2}+\frac{\partial u_3}{\partial\theta}\right)+\frac{N^r_{\theta\theta}}{R^2}\left(\frac{\partial u_3}{\partial\theta}-u_\theta\right) \quad (1)$$
$$-k_\theta u_\theta-\frac{p}{R}\left(\frac{\partial u_3}{\partial\theta}-u_\theta\right)=\rho h\frac{\partial^2 u_\theta}{\partial t^2}$$

$$\frac{D}{R^4}\left(\frac{\partial^3 u_\theta}{\partial\theta^3}-\frac{\partial^4 u_3}{\partial\theta^4}\right)-\frac{K}{R^2}\left(\frac{\partial u_\theta}{\partial\theta}+u_3\right)+\frac{N^r_{\theta\theta}}{R^2}\left(\frac{\partial^2 u_3}{\partial\theta^2}-\frac{\partial u_\theta}{\partial\theta}\right) \quad (2)$$
$$-k_3 u_3+\frac{p}{R}\left(\frac{\partial u_\theta}{\partial\theta}+u_3\right)=\rho h\frac{\partial^2 u_3}{\partial t^2}$$

D and K represent the bending and membrane stiffness, respectively. These stiffnesses are expressed as a function of the Young's modulus E and ring thickness h.

$$D=Eh^3/12\ ,\quad K=Eh \quad (3)$$

The internal pressure on the ring causes a circumferential pretension in the ring. $N^r_{\theta\theta}$ $(\approx pR)$ represents the pretension force resultant in the ring per unit width of the ring [3].
Three assumptions were made to obtain the equations of motion. Firstly, transverse shear deflections of the ring are neglected. Secondly, the stress component acting in the normal direction to the neutral surface is neglected. At last, the Love simplifications for thin shells are applied [2]. This implies that the shell in-plane displacements vary linearly through the shell thickness and that the out-of plane deformation is constant through the shell thickness.

Natural frequencies

The first modes of a flexible ring on elastic foundation are modes in which the ring mainly translates or rotates as a rigid structure. Three of these modes, which are shown in figure 2, will be used to calculate the sidewall stiffness of the presented tyre model.

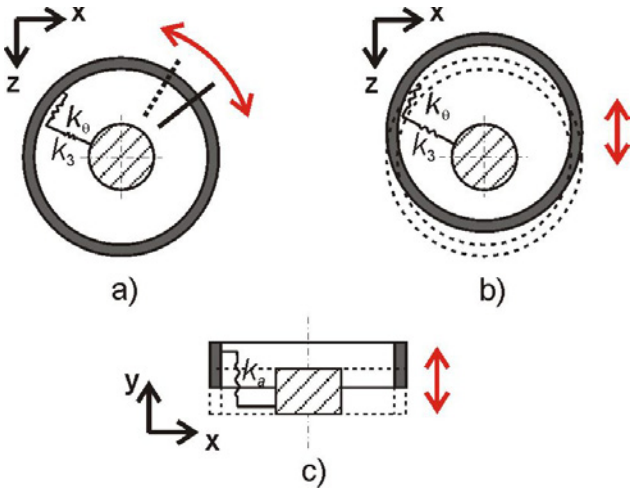

Figure 2: Rigid ring modes. (a) torsional mode; (b) (1,0) mode; (c) axial mode.

At the torsional resonance, the ring rotates as a rigid structure around the lateral axis. The natural frequency of this mode is derived from the two equations of motion and can be written as [3]:

$$\omega_{torsion}^2 = k_\theta / \rho h \tag{4}$$

At the (1,0) resonance, the ring translates as an almost perfectly rigid structure in the plane of the radial and tangential stiffness. The natural frequency of this mode can approximately be calculated as:

$$\omega_{(1,0)}^2 \approx (k_3 + k_\theta) / 2\rho h \tag{5}$$

At the axial resonance, the ring translates as a rigid structure along the lateral axis. The natural frequency of this mode cannot be derived from equations (1) and (2) because the lateral motion is not included in these equations. However, the system can be considered as a single degree of freedom spring-mass system. The axial elastic foundation k_a acts as stiffness and the rigid ring acts as mass. The resonance frequency of the axial mode becomes:

$$\omega_{axial}^2 = k_a / \rho h \tag{6}$$

Development of the structural tyre model

This section describes the finite element based structural tyre model of an unloaded tyre, clamped at the wheel centre. The model is applied to a smooth (slick) tyre of size 205/55R16. The model is implemented in ABAQUS and includes a submodel of the wheel and the air cavity.

Wheel submodel

The dynamic interaction between tyre and wheel has an effect on the vehicle NVH [4]. Consequently, the dynamic behaviour of the steel wheel with rim diameter 16" is included in the tyre model. The geometry of the wheel is modelled in detail because the flexibility of rim and disk are highly influenced by their complex shape. The wheel is discretized in the finite element model by 4-node shell elements and an eigenvalue analysis was performed on the wheel model, clamped at the spindle. The first four resonances were found at 167 Hz, 210 Hz, 368 Hz and 454 Hz. These frequencies are within 7% of the eigenfrequencies measured in an experimental modal analysis on the wheel, clamped at the spindle.

Treadband ring submodel

A radial tyre is composed of radial plies (carcass) that are enclosed by a steel reinforced belt and tread layer. Due to the orientation of the rubberized plies and the steel wires in the belt, the tyre treadband exhibits orthotropic behaviour. In the presented tyre model, the treadband is modelled as an isotropic three-dimensional ring. Despite this drastic simplification, the tyre model exhibits acceptable accuracy in the frequency range of interest, as will be shown in the results and validation section of this paper.

The non-linear static material behaviour of the ring is described by the Neo-Hookean hyperelastic material model. This model is applicable for incompressible and nearly incompressible materials and is commonly used when no accurate material data is available. The dynamic behaviour of rubberlike materials is often characterised by a complex Young's modulus $(E^* = E' + iE'')$. The ratio between imaginary and real part of the complex Young's modulus is referred to as the loss factor η and is a measure for the damping. In this tyre model, the material properties of the treadband are considered to be frequency independent. This corresponds to proportional hysteretic damping and is a commonly used assumption for structure-borne sound applications in the frequency range of interest. The values for the loss factor and the Poisson's ratio are obtained from literature [5]. The elastic storage modulus is tuned by adjusting its value in order to achieve a good correspondence between modelled and measured dynamic response. Table 1 lists the material parameters of the treadband ring. The ring is discretized in the finite element model by 4-node shell elements. The elements allow transverse shear deformation and account for finite membrane strains and arbitrarily large rotations. 90 elements are used in the circumferential direction and 12 elements in the axial direction.

Parameter	Description	Value
E'	Elastic storage modulus	4.5 10^8 N/m^2
η	Loss factor	0.15
ν	Poisson ratio	0.45
ρ	Density	1452 kg/m^3

Table 1: Material parameters of the treadband ring submodel.

Tyre sidewall submodel

The tyre sidewalls are approximated by distributed linear spring-damper systems in radial, tangential and axial direction. The elastic foundation is distributed along the circumference at both edges of the treadband ring. An experimental modal analysis on the unloaded tyre, clamped at the spindle, is performed in order to determine the modal parameters of the torsional, (1,0) and axial tyre resonance.

Equation (7) describes the relation between the undamped natural frequency Ω, damped natural frequency ω and damping ratio ξ for a single degree of freedom system.

$$\omega = (\sqrt{1-\xi^2})\Omega \quad with \quad \xi = \frac{c}{2\sqrt{k\,m}} \;;\; \Omega = \sqrt{\frac{k}{m}} \qquad (7)$$

Equations (4), (5) and (6) are used to calculate the sidewall stiffness from the undamped natural frequency of the torsional, (1,0) and axial mode, respectively. Table 2 lists the calculated distributed linear spring constants k and viscous damping constants c of the sidewall. Unlike the real tyre sidewall, the presented simplified sidewall model has no mass. Therefore, half of the sidewall mass is assigned to both the treadband ring and the wheel rim.

Parameter	Value
k_3 , c_3	9.0 10^6 N/m^3 , 885 N s/m^3
k_θ , c_θ	4.47 10^6 N/m^3 , 1222 N s/m^3
k_a , c_a	1.80 10^6 N/m^3 , 227 N s/m^3

Table 2: Sidewall stiffness and damping constants (values per unit of ring area).

Air cavity submodel

The tyre structural behaviour is significantly affected by the presence of the inner air cavity. The air cavity is discretized using 8-node linear brick acoustic elements and is coupled to the structural mesh of the wheel and treadband ring (Figure 4a). The sidewalls of the cavity are considered to be acoustically rigid. The values of the bulk modulus and the density of air are taken to be 450 kPa and 3.818 kg/m^3, respectively, and represent the properties of air at a temperature of 20 °C and a relative pressure of 2.2 10^5 Pa. The cavity model does not include a damping definition. Typically, the loss factor for the air in the tyre is a factor 100 smaller than the loss factor of the tyre tread.

Tyre-wheel assembly

Figure 4b shows the fully assembled tyre model. For clarity, the cavity mesh is not depicted. First, a static analysis of the tyre inflation is performed. The spindle-wheel interface is clamped and the tyre is inflated to 2.2 10^5 Pa in a geometric non-linear analysis. This pressure loading induces a circumferential pretension in the ring which significantly contributes to the tyre stiffness. Besides the circumferential tension, the tyre treadband is also subjected to an axial tension. This tension is not induced by the inflation pressure in the model and therefore this tension will be applied as an external loading. The calculation of the axial tension is based on a model in which the sidewall is represented as an inextensible membrane with circular section [3]. The axial tensile force on the ring per unit circumferential length $N_{yy}^r\ (= p\,h_s/2)$ is a function of the sidewall height h_s and inflation pressure p .

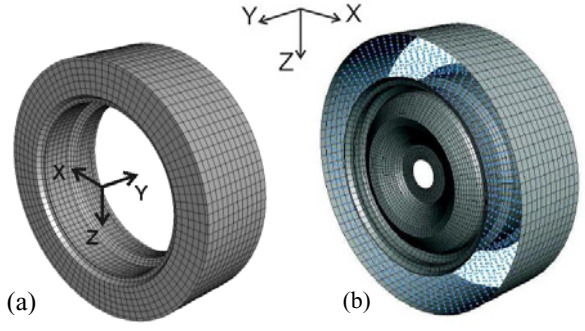

Figure 4: (a) Acoustic mesh.
(b) Fully assembled tyre-wheel model.

Results and validation

After the static analysis in which the tyre is inflated, an eigenvalue analysis is performed in which the first 80 undamped eigenvalues of the tyre model are calculated. This analysis is followed by a complex eigenvalue extraction, based on the Lanczos subspace projection method. Comparison of the calculated damped natural frequencies with the measured natural frequencies shows that the calculated natural frequencies are underestimated. This is a result of the parametrization of the tyre sidewall since the flexibility of the wheel and the structural-acoustic coupling are not taken into account in the analytical ring model. Therefore, the sidewall stiffness values have to updated independently in order to obtain the correct natural frequencies for the torsional, (1,0) and axial mode. Here, the axial, tangential and radial stiffness had to be increased by 13%, 4.5% and 34%, respectively.

Figure 5 reveals that the calculated and measured modes show good agreement. The calculated eigenfrequencies are within 5 % of the measured eigenfrequencies. All calculated modes were identified in the modal test and vice versa. Modes that involve bending of the belt in axial direction cannot be described accurately by the model since the sidewall dynamic behaviour of these modes deviates too much from a spring-damper system.

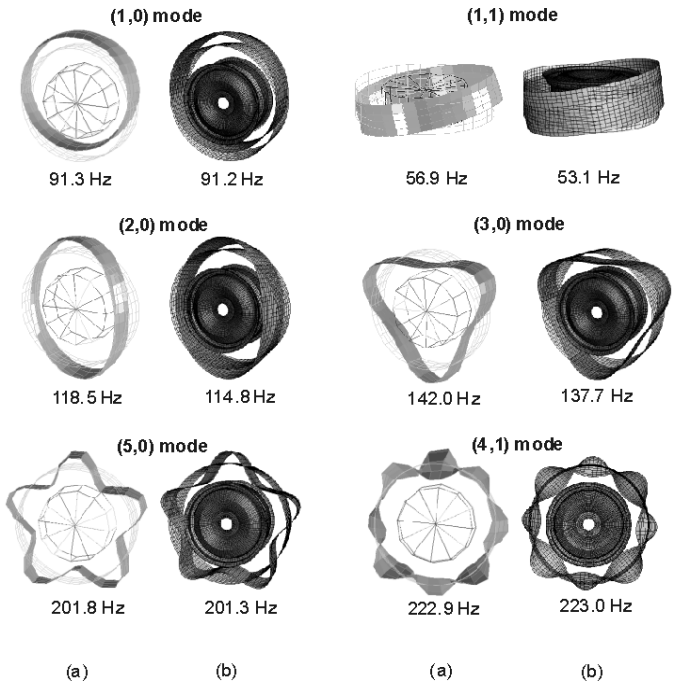

Figure 5: Comparison between measured (a) and calculated (b) mode shapes.

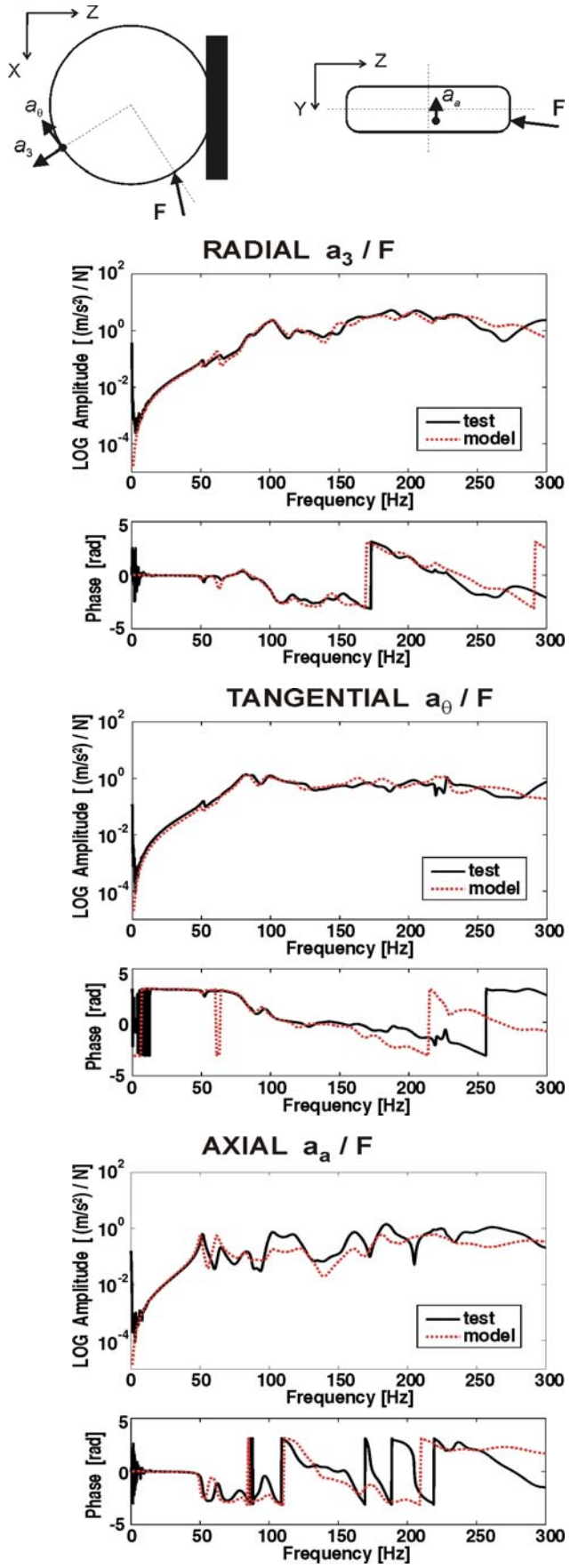

Figure 6: Magnitude and phase of a loaded tyre inertance FRF. Measured (solid) and calculated (dashed).

Since the model is physical, it can also be used to predict the dynamic behaviour under different operating conditions, such as loading and rotation. The above described tyre model is subjected to a static deformation of 16 mm due to the contact with a flat road surface. The hyperelastic material definition and large deformations require that a non-linear FE method is used to simulate the tyre loading. In order to describe the contact accurately, the mesh is refined in the contact patch region. A Coulomb friction coefficient μ of 0.5 is used since the tyre is loaded against a dry smooth steel surface.

The steady-state linearized response of the tyre-wheel model to a harmonic point excitation at the treadband is calculated up to 300 Hz. Figure 6 shows the comparison between the calculated and measured frequency response function in radial, tangential and axial direction. The excitation and response position are shown above the graphs. The agreement between measured and calculated FRF's is good, except for the axial direction. Since the excitation in this direction is limited, a small misalignment of the shaker has a significant effect on the response in this direction.

Conclusions

The presented model is valid below the cut-on of the first treadband axial bending mode; unlike most ring models that are limited to in-plane modes only. The fully assembled tyre model includes a wheel and air cavity model, which is necessary to describe all physical phenomena in the frequency range of interest. This makes the model suitable for the prediction of structure borne interior tyre/road noise. The parametrization of the model is based on simple geometrical properties of the tyre and the experimental modal parameters of three tyre modes. Despite the drastic, well considered simplifications, comparison between measured and calculated responses shows that the tyre-wheel model describes the dynamic behaviour with acceptable accuracy. Since the model is physical, it can also be applied to predict the dynamic behaviour under different operating conditions, such as loading and rotation. In this paper the loaded tyre response is calculated and validated.

References

[1] F. De Coninck, Multi-axial road reproductions for non-linear road noise models. PhD thesis, Katholieke Universiteit Leuven, Belgium, 2007.

[2] W. Soedel, Vibrations of shells and plates. Marcel Decker, New York, Third Edition, 2004.

[3] P. Kindt, P.Sas, W. Desmet, Three-dimensional Ring Model for the Prediction of the Tyre Structural Dynamic Behaviour, Proceedings of ISMA 2008 conference, Leuven, pp 4155-4170.

[4] E. J. Ni, D.S. Snyder, D.S. Walton et al., Radiated Noise from Tire/Wheel Vibration, Tire Science and Technology, TSTCA 25(1), 1997, pp 29-42 .

[5] R.J. Pinnington, A.R. Briscoe, A wave model for a pneumatic tyre belt. Journal of Sound and Vibration 253 (5), 2002, pp 941-959.